Increased peripheral lipid clearance in an animal model of amyotrophic lateral sclerosis[S]

Anissa Fergani,[*,†] Hugues Oudart,[§] Jose-Luis Gonzalez De Aguilar,[*,†] Bastien Fricker,[*,†] Frédérique René,[*,†] Jean-François Hocquette,[**] Vincent Meininger,[††] Luc Dupuis,[1,*,†] and Jean-Philippe Loeffler[*,†]

Institut National de la Santé et de la Recherche Médicale,* U692, Laboratoire de Signalisations Moléculaires et Neurodégénérescence, Strasbourg, F-67085 France; Université Louis Pasteur,† Faculté de Médecine, Unité Mixte de Recherche S692, Strasbourg, F-67085 France; Centre d'Ecologie et Physiologie Energétiques,§ Unité Propre de Recherche 9010, Centre National de la Recherche Scientifique, 67087 Strasbourg Cedex, France; Equipe Croissance et Metabolismes du Muscle,** Unite de Recherches sur les Herbivores, Institut National de la Recherche Agronomique, Centre de Clermont-Ferrand/Theix, 63122 St Genes-Champanelle, France; and Fédération des Maladies du Système Nerveux,†† Centre Référent Maladie Rare Sclerose Lateral Amyotrophique, Hôpital de la Pitié-Salpêtrière, 75651 Paris, France

Abstract Amyotrophic lateral sclerosis (ALS) is the most common adult motor neuron disease, causing motor neuron degeneration, muscle atrophy, paralysis, and death. Despite this degenerative process, a stable hypermetabolic state has been observed in a large subset of patients. Mice expressing a mutant form of Cu/Zn-superoxide dismutase (mSOD1 mice) constitute an animal model of ALS that, like patients, exhibits unexpectedly increased energy expenditure. Counterbalancing for this increase with a high-fat diet extends lifespan and prevents motor neuron loss. Here, we investigated whether lipid metabolism is defective in this animal model. Hepatic lipid metabolism was roughly normal, whereas gastrointestinal absorption of lipids as well as peripheral clearance of triglyceride-rich lipoproteins were markedly increased, leading to decreased postprandial lipidemia. This defect was corrected by the high-fat regimen that typically induces neuroprotection in these animals. Together, our findings show that energy metabolism in mSOD1 mice shifts toward an increase in the peripheral use of lipids. This metabolic shift probably accounts for the protective effect of dietary lipids in this model.—Fergani, A., H. Oudart, J-L. Gonzalez De Aguilar, B. Fricker, F. René, J-F. Hocquette, V. Meininger, L. Dupuis, and J-P. Loeffler. **Increased peripheral lipid clearance in an animal model of amyotrophic lateral sclerosis. *J. Lipid Res.* 2007.** 48: **1571–1580.**

Supplementary key words plasma lipoproteins • neurodegeneration • motor neuron • low density lipoprotein • high density lipoprotein • liver metabolism • intestinal absorption • skeletal muscle

Neurodegenerative diseases have long been considered to be the result of locally restricted injury to specific neurons, the loss of which represents both the origin and the end of the pathological process. However, this "cell-autonomous injury" hypothesis does not seem to hold true for disorders in which neurodegeneration would be caused by the combined action of a series of defects arising at the level of the whole organism, eventually leading to a very selective cell death. Although still poorly understood, peripheral metabolic abnormalities, as shown to occur in several neurodegenerative diseases (1–5), could participate in the neurodegenerative process (6, 7).

Amyotrophic lateral sclerosis (ALS) is a neurodegenerative disease characterized by the progressive loss of motor neurons in the spinal cord, brain stem, and motor cortex. Although tremendous efforts have been devoted to explaining ALS pathogenesis, why motor neurons selectively die in this condition is still unsolved (8, 9). Animal models of ALS displaying the major features of the human disease are transgenic mice overexpressing mutant forms of Cu/Zn-superoxide dismutase (SOD1) (10–12), a free radical-scavenging enzyme that protects cells against oxidative stress and is mutated in a subset of patients with autosomal dominantly inherited ALS (13). Studies using these mice have postulated that mutant superoxide dismutase (mSOD1) triggers ALS by a non-cell-autonomous mechanism involving not only motor neurons themselves but also other cells such as astrocytes and microglia (14, 15).

Beyond the neuromuscular system, we recently observed systemic abnormalities occurring in animal models of ALS (6, 16). mSOD1 mice are leaner than wild-type littermates, and their fat pads gradually deplete as a result of a prominent hypermetabolic trait mainly of muscular origin (6).

Manuscript received 12 January 2007.

Published, JLR Papers in Press, April 16, 2007.
DOI 10.1194/jlr.M700017-JLR200

[1] To whom correspondence should be addressed.
e-mail: ldupuis@neurochem.u-strasbg.fr

[S] The online version of this article (available at http://www.jlr.org) contains supplementary data in the form of a table.

In agreement with these findings, higher resting energy expenditure has also been observed in a large subset of ALS patients (17, 18). Moreover, a significant percentage of patients present with glucose intolerance and increased rates of muscle glucose uptake, oxygen consumption, and lactate output, indicating the presence of marked abnormalities in carbohydrate metabolism in muscle tissue (19). These metabolic alterations that, at least in mice, precede motor neuron death are not only associated with but also contribute to the neurodegenerative process, because it has been shown in mSOD1 mice that increasing the energy content of the diet prolongs lifespan and maintains motor neuron numbers (6, 20), whereas restricting calorie intake hastens the disease (21).

The origin of the systemic defects in mSOD1 mice and their contribution to the pathology of ALS patients need to be elucidated. Given that a highly energetic fat regimen protects against the disease in animal models, we hypothesize that compensation of as yet unidentified disturbances in lipid metabolism could account for the benefits of such a regimen. In the search for these lipid disturbances, we show here that mSOD1 mice present with decreased postprandial lipidemia characterized by increased peripheral clearance of triglyceride (TG)-rich lipoproteins, probably caused by skeletal muscle hypermetabolism. This hypolipidemia was reversed by the neuroprotective high-fat regimen. Together, our findings show that energy metabolism in mSOD1 mice shifts toward an increase in the peripheral use of lipids. This metabolic shift probably accounts for the protective effect of dietary lipids in this model.

MATERIALS AND METHODS

Animals

Transgenic female mice with the G86R murine SOD1 mutation were maintained in a FVB background and maintained with their nontransgenic age-matched female littermates on a 12 h light/dark cycle. They were fed a chow diet (A04; UAR, Epinay sur Orge, France) unless stated otherwise and had free access to water. The high-fat diet consisted of A04 complemented with 20% butter fat. Transgenic mice expressing the human G93A SOD1 mutation were kindly provided by Faust Pharmaceuticals.

Lipid measurements and lipoprotein fractionation

Tail vein blood was collected in heparinized capillary tubes, placed on ice, and centrifuged at 3,000 *g* at 4°C. Plasma levels of TGs, cholesterol, and total lipids were determined with Randox (Crumlin, UK) kits TR213, CH200, and TL100, respectively. The TG TR213 kit is an enzymatic kit based upon the hydrolysis of TGs in glycerol and fatty acids, the glycerol produced being oxidized to reach H_2O_2, which oxidizes 4-aminophenazone and 4-chlorophenol to reach a colored quinoneimine compound. The cholesterol CH200 kit is based upon the oxidation of cholesterol to cholestene 3-one and H_2O_2 by the cholesterol oxidase. The H_2O_2 produced is then dosed upon the same principle as with the TR213 kit. In the CH200 kit, the enzymatic reagent also includes cholesterol esterase, thus allowing the dosage of not only free but also esterified cholesterol. Both TR213 and CH200 kits yielded results in our hands similar to those obtained in a certified clinical biochemistry laboratory (data not shown). The TL100 kit is based upon the reaction of lipids with sulfuric acid, phosphoric acid, and vanillin to form a pink complex. This kit was able to accurately detect exogenous TGs added in serum (data not shown). Moreover, this kit yielded results consistent with those obtained using gravimetric detection of lipids after Folch extraction (data not shown). In all cases, a five point standard curve was performed using the standards provided in the kits, and results were analyzed only if the correlation coefficient of the standard curve was >0.995. Plasma concentrations were calculated using the equation of the regression line as calculated by Excel (Microsoft). In our hands, the intradosage variability of these three kits was <5%. Plasma lipoprotein profiling was performed by the Clinical Mouse Institute (Strasbourg, France) by fast-performance liquid chromatography (FPLC) on a Dionex (Sunnyvale, CA) apparatus.

Lipid and glucose intestinal absorption

Lipid and glucose uptake rates into the small intestine were determined using the in vivo perfused intestinal segments technique (22). Normally fed mice were anesthetized and placed on a heated (37°C) surgical table. After performing a laparotomy, a 10 cm segment of the small intestine was cannulated and the luminal contents were removed by gently flushing with saline solution at 37°C. An intestinal loop was cannulated and a recirculating perfusion was started at a flow rate of 2 ml/min with Intralipid® solution (4%) (Pharmacia, Strasbourg, France) at 37°C for TG uptake. TG and NEFA concentrations were estimated in the luminal contents using Randox kits TR213 and FA115, respectively. For glucose uptake, a saline solution at 37°C containing 5 mM glucose was perfused. The absorption rate was calculated as the difference between the initial and final glucose concentrations using a glucometer (Accu check; Roche, Basel, Switzerland) according to the manufacturer's instructions.

Gastric emptying and intestinal transit

Gastric emptying time and intestinal transit were determined using methylene blue as a tracer dye. Briefly, after a 4 h fast, mice were gavaged with 0.1 ml of methylene blue/10% dextrose solution and euthanized at 30 min after gavage. The stomach was clamped above the esophageal sphincter and below the pylorus to prevent leakage of the dye. Stomachs were cut and immediately homogenized in 10 ml of 0.1 M NaOH. After clearing steps by centrifugation, optical density at 562 nm of the supernatant was determined. Gastric emptying was determined as the difference between the measured optical density and that of a group of mice, gavaged in parallel and euthanized at 1 min after gavage. Intestinal transit was determined as the most distal point of migration of methylene blue in the intestine and expressed as a percentage of the total length of the intestine.

RT-PCR analysis

Each frozen sample (livers or intestinal mucosa) was placed into a tube containing a 5 mm stainless steel bead (Qiagen, Courtaboeuf, France) and 1 ml of Trizol reagent (Invitrogen, Paisley, UK) and homogenized using a TissueLyser (Qiagen) at 30 Hz for 3 min. RNA was extracted by the chloroform-isopropyl alcohol-ethanol (Sigma, Lyon, France) method and stored at −80°C until use. RNA reverse transcription and SYBR Green real-time PCR assays were performed using the Bio-Rad (Marnes la Coquette, France) iCycler kits and protocols. Primer sequences are available in supplementary Table I. The relative levels of each RNA were normalized to the corresponding 18S RNA levels.

Hepatic VLDL production

After a 4 h fast, mice were injected intravenously into the tail vein with 20 mg of tyloxapol (Sigma) as a 20% solution in PBS buffer. Blood samples were drawn at 0, 60, 120, and 240 min after the tyloxapol injection, and TG concentrations were determined in plasma as described above.

Intragastric fat load

After a 4 h fast, mice were given intragastrically a 400 μl olive oil bolus. Blood samples were drawn at 0, 1, 2, 3, 4, and 5 h after bolus administration, and TG concentrations were determined in plasma as described above.

Histological analysis

Adult mice were intracardially perfused with 4% paraformaldehyde (Sigma). Livers were immediately postfixed in 4% paraformaldehyde for 24 h. Serial sections of 40 μm were obtained by vibratome. To visualize fat vesicles, slides were incubated in Oil Red O solution (0.1% Oil Red O dissolved in isopropanol; Sigma) for 15 min at room temperature and washed with 30% isopropanol (Sigma) and distilled water.

Lipoprotein lipase activity

LPL activity was assessed after homogenization of the tissues in a buffer composed of ammonia-HCl (25 mM), pH 8.2, containing EDTA (5 mM), Triton X-100 (8 g/l), sodium dodecyl sulfate (0.10 g/l), heparin (Sigma; 5,000 IU/l), and peptidase inhibitors (Sigma). Insoluble material was discarded by centrifugation at 20,000 *g* for 20 min at 4°C. As described by Hocquette, Graulet, and Olivecrona (23), rat serum was used as activator and Intralipid® (Pharmacia), into which [^{3}H]triolein (Perkin-Elmer, Jügesheim, Germany) had been incorporated, was used as the substrate. Liberated ^{3}H-labeled free fatty acids were quantified by liquid scintillation.

Statistical analysis

Statistical comparisons of these data were performed using either unpaired Student's *t*-test or one-way ANOVA followed by post hoc Newman-Keuls test, using GraphPad Prism software (version 4). Significance was considered at $P < 0.05$.

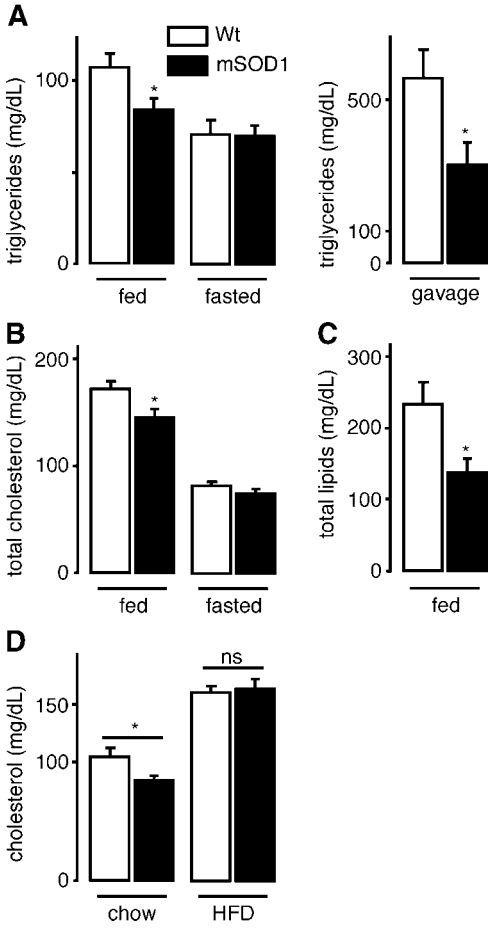

Fig. 1. Decreased postprandial lipidemia in mutant superoxide dismutase 1 (mSOD1) mice. A–C: Plasma triglyceride (TG) (A), cholesterol (B), and total lipids (C) in fed, fasted, and olive oil-gavaged wild-type (Wt; open columns) and mSOD1 (closed columns) mice. n = 10–15 mice for A, B; n = 6 mice for C. * $P < 0.05$ versus the wild type. D: Plasma cholesterol in wild-type and mSOD1 mice fed either the chow diet or the high-fat diet (HFD). n = 10 mice. * $P < 0.05$ versus the corresponding wild type. Error bars represent SEM.

RESULTS

mSOD1 mice display alterations in blood lipid levels

We had previously shown that mSOD1 mice progressively lose their adipose tissue stores and that feeding them a diet enriched in fat prolonged lifespan and rescued motor neurons (6). Here, we observed that asymptomatic mSOD1 mice displayed normal levels of plasma TGs and cholesterol under fasting but showed decreased levels of plasma TG, cholesterol, and total lipids under normal feeding (**Fig. 1A–C**). To ascertain whether the observed decrease in lipid levels in mice was attributable to decreased postprandial lipidemia, we gavaged mice with olive oil and measured TG levels 3 h later. In this experimental setting, we observed an ~2-fold decrease in TG levels compared with wild-type littermates (Fig. 1A, right panel), thus showing that mSOD1 mice, although normolipidemic, present with decreased postprandial lipidemia. To assess whether this defect could be corrected by a high-fat diet, we fed a group of mice 20% butter fat during 4 weeks and evaluated their lipid metabolism. As described previously (6), the high-fat diet reversed the deficit in body mass and repleted adipose tissue stores in mSOD1 mice. In addition, consistent with the documented protective role of this regimen, after 1 month of high-fat diet feeding, only 1 of 10 mice displayed motor troubles, whereas 5 of the 9 mice normally fed showed ALS symptoms (data not shown). The high-fat regimen also abolished the decrease in postprandial cholesterolemia (Fig. 1D). Together, these findings indicate that correcting the decreased postprandial cholesterolemia by feeding mSOD1 mice a high-fat regimen is associated with the attenuation of ALS symptoms.

mSOD1 mice have a defect in TG-rich lipoproteins

The main difference between fasting and feeding in terms of TG is the presence of chylomicrons in the blood of fed animals. Therefore, the decrease in TG in fed but not fasted mSOD1 mice suggested that the chylomicron

system of lipoproteins was affected by the presence of mSOD1. To determine whether other lipoprotein fractions were affected, we performed FPLC to separate the different lipoproteins and quantified their cholesterol contents. We noted a strong decrease (~50%) in VLDL and LDL cholesterol fractions in 75 day old asymptomatic mSOD1 mice but only a slight decrease (<20%) in HDL cholesterol (**Fig. 2A, B**). Thus, the activity of the two lipoprotein systems involved in the transport of lipids toward peripheral tissues, chylomicrons, carrying dietary fats, and VLDL/LDL, transporting endogenously synthesized lipids, appeared decreased in fed asymptomatic mSOD1 mice. The reverse transport of lipids by HDL lipoproteins was only modestly affected. Interestingly, FPLC profiles of wild-type and mSOD1 mice were indistinguishable after 4 h of fasting (Fig. 2C), which suggests that normally fed

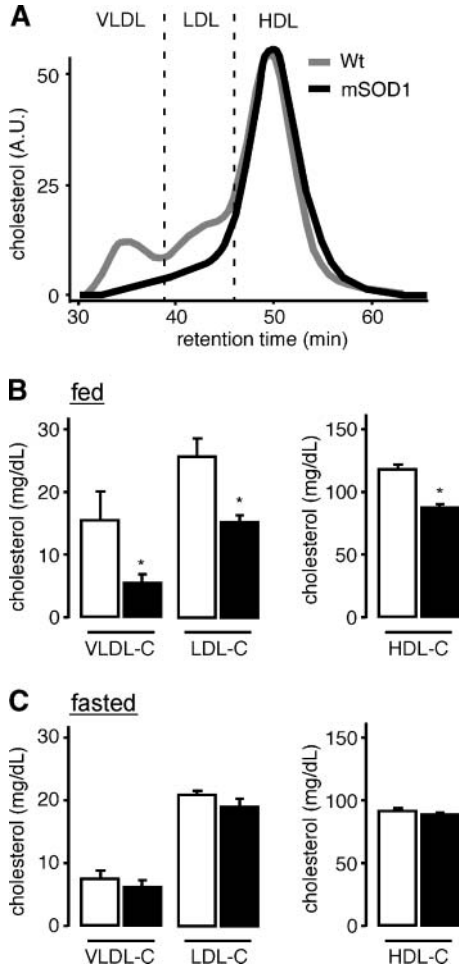

Fig. 2. Fast-performance liquid chromatography (FPLC) fractionation of lipoproteins in mSOD1 mice. A: Representative FPLC profiles of fed wild-type (Wt; gray line) and mSOD1 (black line) mice. Note the depletion of VLDL- and LDL-cholesterol (-C) fractions in mSOD1 mice. A.U., arbitrary units. B: Quantification of the experiments presented in A. n = 6 mice. * $P < 0.05$ versus the wild type. Columns are as in Fig. 1. C: Quantification of FPLC profiles of 4 h-fasted wild-type (open columns) and mSOD1 (closed columns) mice. n = 3 pools of 3 mice. Columns are as in Fig. 1. Error bars represent SEM.

mSOD1 mice behave as if they were fasted, even though they ingested equal or higher amounts of food than their wild-type littermates (6).

Intestinal absorption of lipids is increased in mSOD1 mice

The observed decrease in circulating lipids might be caused by different mechanisms. First, mSOD1 mice might have a decreased food intake. We have already excluded this possibility in asymptomatic mice (6). Second, it is possible that the gastrointestinal system is malfunctioning. This hypothesis is further substantiated by clinical reports of gastrointestinal dysfunction in ALS patients (24). Indeed, mSOD1 was highly expressed in intestinal mucosa, with no age-dependent variations that could explain gastrointestinal dysfunction (**Fig. 3A**). However, gastric emptying and intestinal transit after an oral gavage of methylene blue under fasting conditions appeared unchanged between mSOD1 mice and wild-type littermates (Fig. 3B, C), thus excluding gross gastrointestinal dysfunction. Third, nutrients could be poorly absorbed in the gut. To directly evaluate the absorptive potential of mSOD1 intestine, we used the in vivo perfused intestinal segment technique (Fig. 3D) and perfused either diluted Intralipid®, a TG-rich solution (Fig. 3E, F), or glucose (Fig. 3G). Glucose uptake by the intestine was identical between mSOD1 and wild-type mice and served as control. In contrast, levels of TG in the perfusate after Intralipid® infusion were constantly lower in mSOD1 intestine than in wild-type littermates analyzed in parallel (Fig. 3E). TGs are broken down in the intestine to yield NEFAs, which are the molecular species absorbed by enterocytes (Fig. 3D). Our data then suggested that TGs were degraded more rapidly in mSOD1 mice than in wild-type littermates. To determine whether NEFAs generated from TGs were efficiently absorbed and not accumulated in the gut, we measured them in intestines perfused with a TG-rich solution. In these experiments, the steady-state levels of NEFAs in intestinal perfusates were constantly lower in mSOD1 mice compared with wild-type animals (Fig. 3F), showing that the process of NEFA absorption was not impaired but rather increased in mSOD1 mice. Together with the increased food intake displayed by mSOD1 mice (6) and the absence of gross dysfunction in gastric emptying and intestinal transit, these data rule out the possibility that decreased lipidemia in fed animals was attributable to diminished intestinal absorption.

Liver lipid metabolism is normal in mSOD1 mice

A second mechanism that could account for decreased lipidemia in mSOD1 mice could be a shift in hepatic lipid metabolism, triggered by the high expression of mSOD1 in liver (**Fig. 4A**). Less release of VLDL from liver, caused by decreased TG or cholesterol biosynthesis or by impaired release itself, could in fact explain the decrease of VLDL fractions observed in mSOD1 mice. We measured the mRNA levels of fatty acid synthase (FAS) and sterol-responsive element binding protein 1 (SREBP1), which are involved in hepatic TG biosynthesis (25), and found that

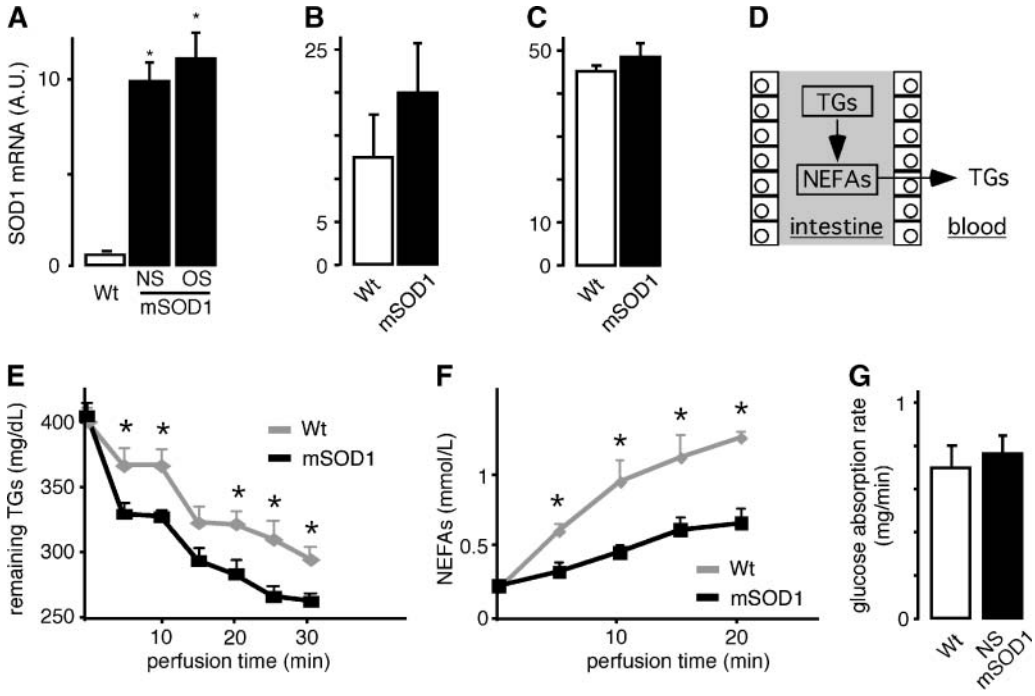

Fig. 3. Increased intestinal absorption in mSOD1 mice. A: Real-time RT-PCR analysis of SOD1 expression in wild-type (Wt; open columns), nonsymptomatic mSOD1 (NS; closed columns), and symptomatic mSOD1 [onset (OS); closed columns]. n = 5 mice. * $P < 0.05$ versus the wild type. mRNA levels are expressed in arbitrary units (A.U.) and are normalized to 18S rRNA. B: Gastric emptying of methylene blue in nonsymptomatic mSOD1 (closed columns) and wild-type (open columns) mice. Animals were euthanized at 30 min after gavage, and the remaining methylene blue in the stomach was assayed spectrophotometrically and compared with that in reference mice euthanized at 1 min after gavage. n = 9 mice. No difference is observed between the two groups. Results are expressed as percentage gastric emptying. C: Intestinal transit of methylene blue in the same mice presented in A. No difference is observed between the two groups. Results are expressed as a percentage of the total length of the intestine. D: Scheme depicting the experimental paradigm used in E and F. TGs are perfused into the intestinal segment, hydrolyzed by intestinal enzymes into NEFAs, absorbed in enterocytes, and reconverted in TG before chylomicron secretion. E, F: Levels of TG and NEFA in the intestinal lumen as a function of time of perfusion. Note that TG decreased faster in mSOD1 mice (black line) than in wild-type mice (gray line) (E), whereas steady-state levels of NEFA remained constantly lower in mSOD1 mice but increased gradually in wild-type mice (F). n = 6–8 mice. * $P < 0.05$ versus the corresponding perfusion time in wild-type mice. G: Glucose absorption rate in wild-type (open column) and nonsymptomatic mSOD1 (closed column) mice. No significant difference is noted between the groups. n = 3–4 mice. Error bars represent SEM.

they were unchanged in presymptomatic mice when hypolipidemia was already detectable (Fig. 4A). In contrast, expression of SREBP1 (and of FAS to a lesser extent) was downregulated in the liver of symptomatic mice, consistent with the documented decrease in insulin levels and the general metabolic shutdown observed in mSOD1 mice at disease onset (6). As far as cholesterol metabolism is concerned, we did not detect any change in the expression of key genes that could compromise cholesterol biosynthesis. Indeed, expression of HMG-CoA reductase, the rate-limiting enzyme in cholesterol biosynthesis, was increased in presymptomatic mice, whereas mRNA levels of SREBP2, a key transcription factor in this pathway, were unchanged before motor symptoms appeared and increased in end-stage mice (Fig. 4A). Together, these data suggest that decreased postprandial lipidemia in mSOD1 mice cannot be ascribed to a deficiency in the expression of key enzymes or transcription factors controlling lipid biosynthesis.

An alternative mechanism leading to decreased postprandial lipidemia could be an increase in lipid catabolism in liver that would generate increased concentrations of ketone bodies. This does not seem to be the case, because mRNA levels of carnitine palmitoyl transferase 1A (CPT1A), the rate-limiting enzyme in fatty acid oxidation, were unchanged in asymptomatic animals (Fig. 4A). In contrast, the increased expression of CPT1A in diseased mice is consistent with the high amounts of ketone bodies found in plasma at this stage (6). Another explanation might be that cholesterol is excreted as bile acid, thus leading to hypolipidemia. However, the expression of cholesterol 7α-hydroxylase (CYP7A1), which is correlated to bile acid biosynthesis (26), was unchanged in presymptomatic mice (Fig. 4A), making it unlikely that an increase in bile acid excretion could be the cause of the early detectable decreased postprandial lipidemia. It should also be noted that treating mSOD1 mice with cholestyramine,

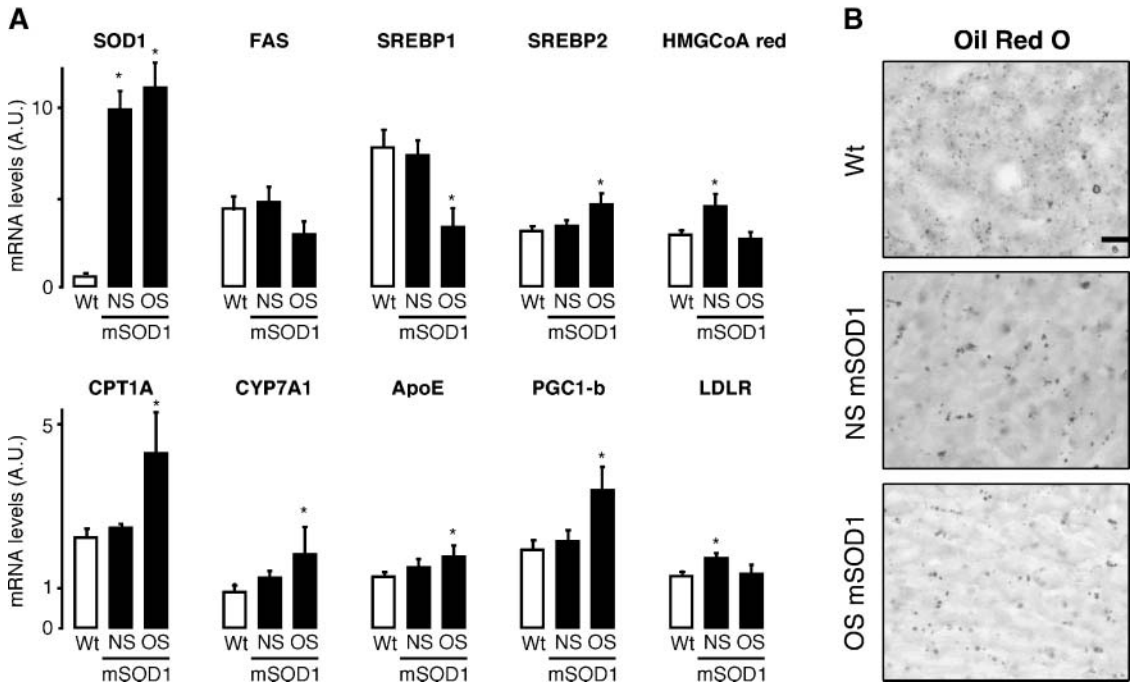

Fig. 4. Hepatic metabolism in mSOD1 mice. A: Real-time RT-PCR analysis of the indicated genes in the liver of wild-type (Wt; open columns) and nonsymptomatic (NS) or symptomatic at onset (OS) mSOD1 (closed columns) mice. n = 7 mice. * $P < 0.05$ versus wild-type mice. mRNA levels are expressed in arbitrary units (A.U.) and are normalized to 18S rRNA. ApoE, apolipoprotein E; CPT1A, carnitine palmitoyl transferase 1A; CYP7A1, cholesterol 7α-hydroxylase; LDLR, low density lipoprotein receptor; PCG1-b, PPAR gamma coactivator 1 beta; SREBP, sterol-responsive element binding protein. B: Representative Oil Red O stainings of liver sections from wild-type and nonsymptomatic or symptomatic at onset mSOD1 mice. n = 3–5 mice. Error bars represent SEM.

a drug known to stimulate bile acid secretion, was able to trigger an increase in CYP7A1 expression, showing that transcription could still be induced in these mice in response to an appropriate stimulus (data not shown). Finally, the expression of genes involved in lipoprotein assembly, such as apolipoprotein E or the transcriptional coactivator PPAR gamma coactivator 1-β, appeared unchanged in presymptomatic mice and increased in diseased animals (Fig. 4A), which further reinforces the notion that lipoprotein assembly is not deficient at the transcriptional level in mSOD1 mice. Interestingly, mRNA levels of the low density lipoprotein receptor (LDLR) were increased at the presymptomatic stage, suggesting that the turnover of LDL might be increased in mSOD1 mice.

Hepatic VLDL assembly and secretion could also be impaired posttranscriptionally, thus leading to hypolipidemia, as occurs when nascent VLDLs are retained in liver. To test whether fats accumulate in the liver of mSOD1 mice, we visualized lipid droplets by Oil Red O staining. As illustrated in Fig. 4B, accumulations of lipids were clearly distinguishable and comparable between wild-type and mSOD1 mice, although an overall fainter stain was observed in end-stage mice. In all, the indirect evidence indicates a normal hepatic lipid metabolism in mSOD1 mice.

TG clearance by peripheral tissues is increased in mSOD1 mice

To directly test whether mSOD1 mouse liver releases VLDL efficiently, we measured hepatic VLDL production under fasting conditions using tyloxapol (Triton WR-1339), a detergent that coats lipoprotein complexes and thus impairs their peripheral clearance. In tyloxapol-injected mice, the rate of increase in plasma TG is correlated to the biosynthesis of VLDL in liver. The increasing concentrations of TG in plasma were almost identical in mSOD1 and wild-type mice (**Fig. 5A**), showing that VLDL production was not impaired in the transgenic animals. Together, these data show that decreased postprandial lipidemia in presymptomatic mSOD1 mice cannot be explained by the altered capacity of liver to synthesize TG and release them in the form of VLDL into the circulation.

To examine whether the decrease in plasma TG-rich lipoproteins was attributable to increased peripheral uptake of lipids, we performed a fat-loading test by administering TG intragastrically in the form of olive oil after a 4 h fast. Initial TG levels were similar in mSOD1 and wild-type mice, consistent with previous results (Fig. 5B). TG levels increased gradually and comparably between the two groups during the first 2 h after gavage, which further confirms that intestinal absorption of fat as well as chylomicron production by the intestine are roughly normal in transgenic animals (Fig. 3). Later, the clearance of TG, represented by the decreasing segments of the curves in Fig. 5B, was faster in mSOD1 mice than in wild-type littermates. These data reflect the increased ability of mSOD1 mice to metabolize TG. We propose that this is likely to be the cause of the decreased postprandial lipidemia observed in these animals.

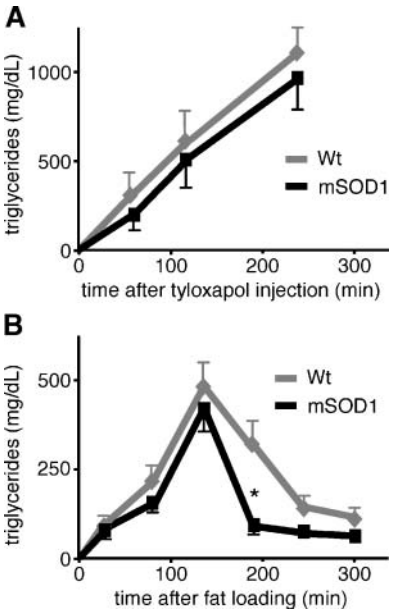

Fig. 5. Lipoprotein production and clearance in mSOD1 mice. A: Determination of VLDL-TG production rates in wild-type (Wt; gray line) and nonsymptomatic mSOD1 (mSOD1; black line) mice. After a 4 h fast, tyloxapol was injected intravenously and plasma samples were assayed for TG content at the indicated time points. Note that TG increases are indistinguishable between the two groups of animals, showing that VLDL secretion is normal in mSOD1 animals. n = 6 mice. B: Plasma TG content during a fat-loading test in wild-type (gray line) and nonsymptomatic mSOD1 (black line) mice. n = 6 mice. After a 4 h fast, mice were gavaged with 400 μl of olive oil. Before and after fat loading, blood was collected serially and plasma TG levels were measured. The experiments was repeated three times with independent cohorts of mice and yielded similar results. * $P < 0.05$ versus control littermates. Error bars represent SEM.

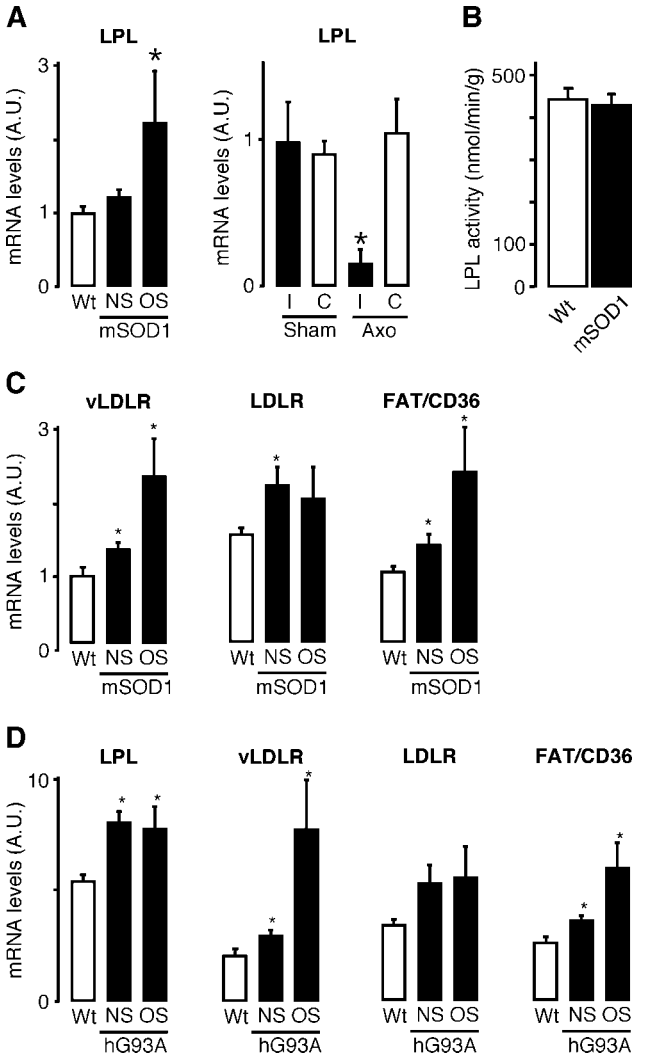

Fig. 6. Expression of genes involved in lipid uptake in skeletal muscles of mSOD1 mice. A: Real-time RT-PCR analysis of LPL expression in the hind limb skeletal muscles of wild-type (Wt; open columns) and nonsymptomatic (NS) or symptomatic at onset (OS) mSOD1 (closed columns) mice. mRNA levels of LPL were also measured in axotomized mice (Axo) at the ipsilateral (I) and contralateral (C) sides of the lesion. Sham-operated mice served as controls. * $P < 0.05$ versus corresponding wild-type mice at the same time point. mRNA levels are expressed in arbitrary units (A.U.) and are normalized to 18S rRNA. B: Total LPL activity in hind limb muscles of wild-type (open column) and nonsymptomatic mSOD1 (closed column) mice. n = 8 mice. No significant difference was noted between the two groups. C: Real-time RT-PCR analysis of the indicated genes in the hind limb skeletal muscles of wild-type (open columns) and nonsymptomatic or symptomatic at onset mSOD1 (closed columns) mice. * $P < 0.05$ versus corresponding wild-type mice. mRNA levels are expressed in arbitrary units and are normalized to 18S rRNA. vLDLR, very low density lipoprotein receptor. D: Real-time RT-PCR analysis of the indicated genes in the hind limb skeletal muscles of wild-type (open columns) and nonsymptomatic or symptomatic at onset G93A (closed columns) mice. n = 6 mice. * $P < 0.05$ versus corresponding wild-type mice. mRNA levels are expressed in arbitrary units and are normalized to 18S rRNA. Error bars represent SEM.

Gene expression changes suggest muscle as the origin of increased lipid peripheral uptake

Because we had previously shown that skeletal muscle is characterized by a hypermetabolic trait in mSOD1 mice (6) and is one of the most important tissues that captures lipids, we tested whether muscle could be the site of increased lipid uptake. Surprisingly, the expression levels of LPL were unchanged in asymptomatic mSOD1 mice and increased in symptomatic animals (**Fig. 6A**, left panel). This late increase does not seem to be the result of denervation, because LPL mRNA levels did not increase but rather decreased after sciatic nerve axotomy (Fig. 6A, right panel). To test whether muscle lipid uptake could be promoted by increased LPL activity, we measured total LPL enzymatic activity but did not find any difference between mSOD1 and wild-type mice (Fig. 6B). However, mRNA levels of several other genes involved in lipoprotein clearance, such as LDLR, very low density lipoprotein receptor (VLDLR), and the fatty acid transporter FAT/CD36, were augmented in the muscles of both presymptomatic and diseased mice (Fig. 6C), which supports the hypothesis that muscle tissue is a primary site of increased lipid consumption in mSOD1 mice. To exclude the possibility that

our observations could result from a transgenic artifact, we also measured the expression of LPL, VLDLR, LDLR, and FAT/CD36 in muscles of G93A mice, another transgenic line overexpressing a human mutant SOD1 (11). We found in these mice not only the previously observed upregulation of VLDLR and FAT/CD36 but also increased levels of LPL mRNA in presymptomatic mice (Fig. 6D). Together, these data suggest that the decreased postprandial lipidemia in mSOD1 mice is driven by the increased clearance of TG in peripheral tissues, particularly skeletal muscle.

DISCUSSION

We show here that energy metabolism of mSOD1 mice, an animal model of ALS, is shifted toward an increased peripheral use of lipids. This metabolic shift probably accounts for the protective effect of dietary lipids in this model.

We had previously shown that mSOD1 mice are afflicted by prominent unbalanced energy homeostasis. In particular, two different mSOD1 mouse lines display increased resting energy expenditure, as determined by indirect calorimetry (6). Importantly, 30–60% of ALS patients also present with hypermetabolism, as determined by the same methodology (17, 18, 27). We then suggested that the origin of this hypermetabolic trait was an increased demand for nutrients in muscle tissue. This hypothesis was supported by increased glucose uptake and altered gene expression of enzymes involved in glucose and lipid use that we observed in muscles of presymptomatic mSOD1 mice (6). Our present data now show that the lipids supplied by normal feeding rapidly disappear from plasma, suggesting muscle hypermetabolism as triggering increased peripheral clearance of TG-rich lipoproteins. This phenomenon, associated with unchanged levels of VLDL secretion by the liver, is likely to account for the postprandial hypolipidemia observed in the transgenic mice.

The results reported here, along with our previous studies (6, 16), support the dysfunction of skeletal muscle metabolism as the cause of the impairment of energy homeostasis in mSOD1 mice. We and others had previously shown mitochondrial dysfunction accompanied by ATP depletion and uncoupling protein 3 upregulation in skeletal muscle of mSOD1 mice (16) and ALS patients (28–31). It is thus probable that this mitochondrial impairment could underlie the increased energy needs of skeletal muscle, as reflected by the increased rates of glucose uptake (6) and TG clearance shown here.

The mechanisms recruited by mSOD1 muscles to increase lipid uptake are not completely understood. We observed the increased expression of enzymes and transporters involved in lipid metabolism, including VLDLR, LDLR, and FAT/CD36, but failed to demonstrate an increase in LPL activity in mSOD1 muscles. In contrast, muscle LPL mRNA levels, although unchanged in presymptomatic G86R mice, appeared increased at disease onset as well as in both presymptomatic and diseased G93A mice, suggesting that LPL might be involved in promoting greater lipid uptake. These results contrast with the transcriptional downregulation of LPL in denervated muscles, which suggests that other mechanisms distinct from pure denervation influence muscle pathology in the transgenic mice.

There are several potential explanations for the lack of an increase in LPL activity in mSOD1 muscles. First, we assayed total LPL activity, although only a fraction of it (i.e., the heparin-releasable fraction) is biologically active. Thus, measurement of total activity could have masked the action of the active LPL. Second, LPL activity in vivo is regulated by numerous factors, in particular plasma proteins, such as apolipoprotein C-II (activator) and apolipoprotein C-III (inhibitor), that are lost in our assay. Third, genes known to increase TG-rich lipoprotein clearance through LPL, such as VLDLR (32–34) and FAT/CD36 (35, 36), were upregulated in presymptomatic mSOD1 mouse muscles. The increased expression of these genes is sufficient to suggest increased lipid uptake in muscle; notably, FAT/CD36 deficiency was recently reported to decrease TG-rich lipoprotein clearance without affecting postheparin LPL activity (35), consistent with a role of CD36 in increasing local LPL activity without increasing either the expression or assayable activity of LPL. Together, our data suggest that LPL activity could actually be increased in mutant SOD1 mouse muscles through yet unknown local factors, which may include CD36. In all, skeletal muscle hypermetabolism is likely to trigger the observed aberrant decreased postprandial lipidemia in mSOD1 mice. In this scenario, the protective potential of a high-fat diet might be interpreted as an increased supply of high-energy nutrients to the muscle, compensating for its dysfunction.

A recent report claimed the lack of involvement of skeletal muscle in mSOD1-triggered pathology (37). The authors used mSOD1 mice (15) whose transgene was flanked by IoxP sequences allowing its excision in skeletal muscle by muscle targeted CRE recombinase expression. However, recombination occurred significantly only in one of the two muscles tested. Most importantly, the efficiency of recombination in respiratory muscles was not provided, although it is thought that their failure triggers the death of the mice. Last, neither motor neuron counting nor neuromuscular junction morphology was provided, thus weakening the conclusions drawn from these experiments. In all, the question of the contribution of skeletal muscle mSOD1 expression remains open. It is clear, however, that skeletal muscle hypermetabolism might also be triggered by mutant SOD1 expression in other cells. Further research is needed to elucidate this point.

Our report gives clues for a nutritional management of ALS patients, suggesting that increasing calorie intake might increase survival and that hypolipidemic drugs such as fibrates, cholestyramine, and statins should be avoided in these patients, because decreasing lipidemia is likely to exacerbate the ALS condition. Contrary to animal models of Parkinson's disease (38) and Huntington's disease (39), in which caloric restriction has been shown to alleviate symptoms, caloric restriction shortens disease duration in mSOD1 mice (21). Our studies in mSOD1 mice suggest

that maintaining body mass index should slow disease progression.

The authors acknowledge the expert technical assistance of Marie José Ruivo, Annie Picchinenna, Nicole Guivier, and David Chadeyron. The authors also acknowledge Dr. Christian Koehl (Laboratoire de Biochimie Générale et Spécialisée, Hôpitaux Universitaires de Strasbourg) and Dr. Andoni Echaniz-Laguna for help with TG and cholesterol dosages. This study was supported by grants from the Association pour l'Etude de la Culture d'Embryons et des Thérapeutiques des Maladies du Système Nerveux, Région Alsace, and the Fondation pour la Recherche Médicale to A.F.; from the Fondation pour la Recherche sur le Cerveau to L.D.; from the Association pour la Recherche sur la Sclérose Latérale Amyotrophique (ARS) to J.-L.G.D.A.; and from the Association Française contre les Myopathies, Alsace Biovalley, the ARS, and the Association pour la Recherche et le Développement de Moyens de Lutte contre les Maladies Neurodégénératives to J.-P.L.

REFERENCES

1. Pedersen, W. A., and E. R. Flynn. 2004. Insulin resistance contributes to aberrant stress responses in the Tg2576 mouse model of Alzheimer's disease. *Neurobiol. Dis.* **17:** 500–506.
2. Pedersen, W. A., P. J. McMillan, J. J. Kulstad, J. B. Leverenz, S. Craft, and G. R. Haynatzki. 2006. Rosiglitazone attenuates learning and memory deficits in Tg2576 Alzheimer mice. *Exp. Neurol.* **199:** 265–273.
3. Bjorkqvist, M., M. Fex, E. Renstrom, N. Wierup, A. Petersen, J. Gil, K. Bacos, N. Popovic, J. Y. Li, F. Sundler, et al. 2005. The R6/2 transgenic mouse model of Huntington's disease develops diabetes due to deficient beta-cell mass and exocytosis. *Hum. Mol. Genet.* **14:** 565–574.
4. Fain, J. N., N. A. Del Mar, C. A. Meade, A. Reiner, and D. Goldowitz. 2001. Abnormalities in the functioning of adipocytes from R6/2 mice that are transgenic for the Huntington's disease mutation. *Hum. Mol. Genet.* **10:** 145–152.
5. Hurlbert, M. S., W. Zhou, C. Wasmeier, F. G. Kaddis, J. C. Hutton, and C. R. Freed. 1999. Mice transgenic for an expanded CAG repeat in the Huntington's disease gene develop diabetes. *Diabetes.* **48:** 649–651.
6. Dupuis, L., H. Oudart, F. Rene, J. L. Gonzalez de Aguilar, and J. P. Loeffler. 2004. Evidence for defective energy homeostasis in amyotrophic lateral sclerosis: benefit of a high-energy diet in a transgenic mouse model. *Proc. Natl. Acad. Sci. USA.* **101:** 11159–11164.
7. Weydt, P., V. V. Pineda, A. E. Torrence, R. T. Libby, T. F. Satterfield, E. R. Lazarowski, M. L. Gilbert, G. J. Morton, T. K. Bammler, A. D. Strand, et al. 2006. Thermoregulatory and metabolic defects in Huntington's disease transgenic mice implicate PGC-1alpha in Huntington's disease neurodegeneration. *Cell Metab.* **4:** 349–362.
8. Pasinelli, P., and R. H. Brown. 2006. Molecular biology of amyotrophic lateral sclerosis: insights from genetics. *Nat. Rev. Neurosci.* **7:** 710–723.
9. Gonzalez de Aguilar, J. L., A. Echaniz-Laguna, A. Fergani, F. René, V. Meininger, J. P. Loeffler, and L. Dupuis. 2007. Amyotrophic lateral sclerosis: all roads lead to Rome. *J. Neurochem.* **101:** 1153–1160.
10. Ripps, M. E., G. W. Huntley, P. R. Hof, J. H. Morrison, and J. W. Gordon. 1995. Transgenic mice expressing an altered murine superoxide dismutase gene provide an animal model of amyotrophic lateral sclerosis. *Proc. Natl. Acad. Sci. USA.* **92:** 689–693.
11. Gurney, M. E., H. Pu, A. Y. Chiu, M. C. Dal Canto, C. Y. Polchow, D. D. Alexander, J. Caliendo, A. Hentati, Y. W. Kwon, and H. X. Deng. 1994. Motor neuron degeneration in mice that express a human Cu,Zn superoxide dismutase mutation. *Science.* **264:** 1772–1775.
12. Wong, P. C., C. A. Pardo, D. R. Borchelt, M. K. Lee, N. G. Copeland, N. A. Jenkins, S. S. Sisodia, D. W. Cleveland, and D. L. Price. 1995. An adverse property of a familial ALS-linked SOD1 mutation causes motor neuron disease characterized by vacuolar degeneration of mitochondria. *Neuron.* **14:** 1105–1116.
13. Rosen, D. R., T. Siddique, D. Patterson, D. A. Figlewicz, P. Sapp, A. Hentati, D. Donaldson, J. Goto, J. P. O'Regan, H. X. Deng, et al. 1993. Mutations in Cu/Zn superoxide dismutase gene are associated with familial amyotrophic lateral sclerosis. *Nature.* **362:** 59–62.
14. Clement, A. M., M. D. Nguyen, E. A. Roberts, M. L. Garcia, S. Boillee, M. Rule, A. P. McMahon, W. Doucette, D. Siwek, R. J. Ferrante, et al. 2003. Wild-type nonneuronal cells extend survival of SOD1 mutant motor neurons in ALS mice. *Science.* **302:** 113–117.
15. Boillee, S., K. Yamanaka, C. S. Lobsiger, N. G. Copeland, N. A. Jenkins, G. Kassiotis, G. Kollias, and D. W. Cleveland. 2006. Onset and progression in inherited ALS determined by motor neurons and microglia. *Science.* **312:** 1389–1392.
16. Dupuis, L., F. di Scala, F. Rene, M. de Tapia, H. Oudart, P. F. Pradat, V. Meininger, and J. P. Loeffler. 2003. Up-regulation of mitochondrial uncoupling protein 3 reveals an early muscular metabolic defect in amyotrophic lateral sclerosis. *FASEB J.* **17:** 2091–2093.
17. Desport, J. C., P. M. Preux, L. Magy, Y. Boirie, J. M. Vallat, B. Beaufrere, and P. Couratier. 2001. Factors correlated with hypermetabolism in patients with amyotrophic lateral sclerosis. *Am. J. Clin. Nutr.* **74:** 328–334.
18. Kasarskis, E. J., S. Berryman, J. G. Vanderleest, A. R. Schneider, and C. J. McClain. 1996. Nutritional status of patients with amyotrophic lateral sclerosis: relation to the proximity of death. *Am. J. Clin. Nutr.* **63:** 130–137.
19. Gonzalez de Aguilar, J. L., L. Dupuis, H. Oudart, and J. P. Loeffler. 2005. The metabolic hypothesis in amyotrophic lateral sclerosis: insights from mutant Cu/Zn-superoxide dismutase mice. *Biomed. Pharmacother.* **59:** 190–196.
20. Mattson, M. P., R. G. Cutler, and S. Camandola. 2007. Energy intake and amyotrophic lateral sclerosis. *Neuromolecular Med.* **9:** 17–20.
21. Pedersen, W. A., and M. P. Mattson. 1999. No benefit of dietary restriction on disease onset or progression in amyotrophic lateral sclerosis Cu/Zn-superoxide dismutase mutant mice. *Brain Res.* **833:** 117–120.
22. Habold, C., C. Foltzer-Jourdainne, Y. Le Maho, J. H. Lignot, and H. Oudart. 2005. Intestinal gluconeogenesis and glucose transport according to body fuel availability in rats. *J. Physiol.* **566:** 575–586.
23. Hocquette, J. F., B. Graulet, and T. Olivecrona. 1998. Lipoprotein lipase activity and mRNA levels in bovine tissues. *Comp. Biochem. Physiol. B Biochem. Mol. Biol.* **121:** 201–212.
24. Toepfer, M., C. Folwaczny, A. Klauser, R. L. Riepl, W. Muller-Felber, and D. Pongratz. 1999. Gastrointestinal dysfunction in amyotrophic lateral sclerosis. *Amyotroph. Lateral Scler. Other Motor Neuron Disord.* **1:** 15–19.
25. Eberle, D., B. Hegarty, P. Bossard, P. Ferre, and F. Foufelle. 2004. SREBP transcription factors: master regulators of lipid homeostasis. *Biochimie.* **86:** 839–848.
26. Russell, D. W. 2003. The enzymes, regulation, and genetics of bile acid synthesis. *Annu. Rev. Biochem.* **72:** 137–174.
27. Desport, J. C., F. Torny, M. Lacoste, P. M. Preux, and P. Couratier. 2005. Hypermetabolism in ALS: correlations with clinical and paraclinical parameters. *Neurodegener Dis.* **2:** 202–207.
28. Echaniz-Laguna, A., J. Zoll, E. Ponsot, B. N'guessan, C. Tranchant, J. P. Loeffler, and E. Lampert. 2006. Muscular mitochondrial function in amyotrophic lateral sclerosis is progressively altered as the disease develops: a temporal study in man. *Exp. Neurol.* **198:** 25–30.
29. Vielhaber, S., K. Winkler, E. Kirches, D. Kunz, M. Buchner, H. Feistner, C. E. Elger, A. C. Ludolph, M. W. Riepe, and W. S. Kunz. 1999. Visualization of defective mitochondrial function in skeletal muscle fibers of patients with sporadic amyotrophic lateral sclerosis. *J. Neurol. Sci.* **169:** 133–139.
30. Vielhaber, S., D. Kunz, K. Winkler, F. R. Wiedemann, E. Kirches, H. Feistner, H. J. Heinze, C. E. Elger, W. Schubert, and W. S. Kunz. 2000. Mitochondrial DNA abnormalities in skeletal muscle of patients with sporadic amyotrophic lateral sclerosis. *Brain.* **123:** 1339–1348.
31. Krasnianski, A., M. Deschauer, S. Neudecker, F. N. Gellerich, T. Muller, B. G. Schoser, M. Krasnianski, and S. Zierz. 2005. Mitochondrial changes in skeletal muscle in amyotrophic lateral sclerosis and other neurogenic atrophies. *Brain.* **128:** 1870–1876.
32. Espirito Santo, S. M., P. C. Rensen, J. R. Goudriaan, A. Bensadoun, N. Bovenschen, P. J. Voshol, L. M. Havekes, and B. J. van Vlijmen. 2005. Triglyceride-rich lipoprotein metabolism in unique VLDL receptor, LDL receptor, and LRP triple-deficient mice. *J. Lipid Res.* **46:** 1097–1102.

33. Goudriaan, J. R., S. M. Espirito Santo, P. J. Voshol, B. Teusink, K. W. van Dijk, B. J. van Vlijmen, J. A. Romijn, L. M. Havekes, and P. C. Rensen. 2004. The VLDL receptor plays a major role in chylomicron metabolism by enhancing LPL-mediated triglyceride hydrolysis. *J. Lipid Res.* **45:** 1475–1481.
34. Yagyu, H., E. P. Lutz, Y. Kako, S. Marks, Y. Hu, S. Y. Choi, A. Bensadoun, and I. J. Goldberg. 2002. Very low density lipoprotein (VLDL) receptor-deficient mice have reduced lipoprotein lipase activity. Possible causes of hypertriglyceridemia and reduced body mass with VLDL receptor deficiency. *J. Biol. Chem.* **277:** 10037–10043.
35. Drover, V. A., M. Ajmal, F. Nassir, N. O. Davidson, A. M. Nauli, D. Sahoo, P. Tso, and N. A. Abumrad. 2005. CD36 deficiency impairs intestinal lipid secretion and clearance of chylomicrons from the blood. *J. Clin. Invest.* **115:** 1290–1297.
36. Ibrahimi, A., A. Bonen, W. D. Blinn, T. Hajri, X. Li, K. Zhong, R. Cameron, and N. A. Abumrad. 1999. Muscle-specific overexpression of FAT/CD36 enhances fatty acid oxidation by contracting muscle, reduces plasma triglycerides and fatty acids, and increases plasma glucose and insulin. *J. Biol. Chem.* **274:** 26761–26766.
37. Miller, T. M., S. H. Kim, K. Yamanaka, M. Hester, P. Umapathi, H. Arnson, L. Rizo, J. R. Mendell, F. H. Gage, D. W. Cleveland, et al. 2006. Gene transfer demonstrates that muscle is not a primary target for non-cell autonomous toxicity in familial amyotrophic lateral sclerosis. *Proc. Natl. Acad. Sci. USA.* **103:** 19546–19551.
38. Maswood, N., J. Young, E. Tilmont, Z. Zhang, D. M. Gash, G. A. Gerhardt, R. Grondin, G. S. Roth, J. Mattison, M. A. Lane, et al. 2004. Caloric restriction increases neurotrophic factor levels and attenuates neurochemical and behavioral deficits in a primate model of Parkinson's disease. *Proc. Natl. Acad. Sci. USA.* **101:** 18171–18176.
39. Duan, W., Z. Guo, H. Jiang, M. Ware, X. J. Li, and M. P. Mattson. 2003. Dietary restriction normalizes glucose metabolism and BDNF levels, slows disease progression, and increases survival in huntingtin mutant mice. *Proc. Natl. Acad. Sci. USA.* **100:** 2911–2916.